IEEE Access
Multidisciplinary | Rapid Review | Open Access Journal

Received July 22, 2016, accepted August 18, 2016. Date of publication xxxx 00, 0000, date of current version xxxx 00, 0000.

Digital Object Identifier 10.1109/ACCESS.2016.2604323

Truncated-ARQ Aided Adaptive Network Coding for Cooperative Two-Way Relaying Networks: Cross-Layer Design and Analysis

YANPING YANG[1], (Student Member, IEEE), WEI CHEN[2], (Senior Member, IEEE), OU LI[1], QINGWEN LIU[3], (Senior Member, IEEE), AND LAJOS HANZO[4], (Fellow, IEEE)

AQ:1 [1]National Digital Switching System Engineering and Technological R&D Center
[2]Tsinghua University
[3]Tongji University
[4]University of Southampton

Corresponding author: L. Hanzo (lh@ecs.soton.ac.uk)

This work was supported in part by NSFC under Grant 61671269, Grant 61201380, Grant 61322111, and Grant 61321061, in part by the National High Technology Research and Development Program of China (863 Program) under Grant 2012AA121606, in part by the National Basic Research Program of China (973 Program) under Grant 2013CB336600 and Grant 2012CB316000, in part by the Engineering and Physical Sciences Research Council under Project EP/Noo4558/1 and Project EP/L018659/1, in part by the Tsinghua National Laboratory on Information Science and Technology, in part by the European Research Council's Advanced Fellow Grant through the Beam-Me-Up project, and in part by the Royal Society Wolfson Research Merit Award.

ABSTRACT Network coding (NC) constitutes a promising technique of improving the throughput of relay-aided networks. In this context, we propose a cross-layer design for both amplify-and-forward and decode-and-forward two-way relaying based on the NC technique invoked for improving the achievable throughput under specific quality of service requirements, such as the maximum affordable delay and error rate. We intrinsically amalgamate adaptive analog network coding (ANC) and network coded modulation (NCM) with truncated Automatic Repeat reQuest (ARQ) operating at the different open system interconnection layers. At the data-link layer, we design a pair of improved NC-based ARQ strategies based on the stop-and-wait and the selective-repeat ARQ protocols. At the physical layer, adaptive ANC/NCM are invoked based on our approximate packet error ratio. We demonstrate that the adaptive ANC design can be readily amalgamated with the proposed protocols. However, adaptive NC-QAM suffers from an SNR-loss, when the transmit rates of the pair of downlink channels spanning from the relay to the pair of destinations are different. Therefore, we develop a novel transmission strategy for jointly selecting the optimal constellation sizes for both of the relay-to-destination links that have to be adapted to both pair of channel conditions. Finally, we analyze the attainable throughput, demonstrating that our truncated ARQ-aided adaptive ANC/NCM schemes attain considerable throughput gains over the schemes dispensing with ARQ, while our proposed scheme is capable of supporting bidirectional NC scenarios.

INDEX TERMS Cooperative communication, cross-layer design, two-way relaying, network-coded modulation, automatic repeat request.

NOMENCLATURE

TWR	Two-Way Relaying
ARQ	Automatic Repeat reQuest
HARQ	Hybrid ARQ
OSI	Open System Interconnection
PER	Packet Error Ratio
QoS	Quality of Service
AF-TWR	Amplify-and-Forward Two-Way Relaying
DF-TWR	Decoded-and-Forward Two-Way Relaying
NC	Network Coding
NCM	Network-Coded Modulation
AM	Adaptive Modulation
AMC	Adaptive Modulation and Coding
ANC	Analog Network Coding
MA	Multiple Access
BC	Broadcast
DL	Downlink
RN	Relay Node

SN	Source Node
QAM	Quadrature Amplitude Modulation
PSK	Phase Shift Keying
CRC	Cyclic Redundancy Checking
DC	Direct Current
SW-ARQ	Stop-and-Wait ARQ
SR-ARQ	Selective-and-Repeat ARQ
BER	Bit-Error-Rate
AWGN	Additive White Gaussian Noise
SNR	Signal-to-Noise Ratio
CSI	Channel State Information
TDD	Time Division Duplexing
ACK	Acknowledgment
NAK	Negative Acknowledgment
RQ	Retransmission reQuest

NOTATIONS

h_1, h_2, g_1, g_2	channel gains
$M_1, M_2, M_{1ij}, M_{2ij}, M_{1,i}, M_{2,j}$	constellation size for SN1→RN→DN2 (RN→DN2) and SN2→RN →DN1 (RN→DN1) links
$\gamma_i, i = 1, 2$	the received SNRs at DN1 and DN2
$p(\gamma_i), i = 1, 2$	distributions of γ_i
$P_{ij}, P_{rij}, P_1, P_2$	transmit powers at RN or SNs
$\bar{P}_r, \bar{P}$	average transmit power
$P_0^{N_{\gamma_i}^{\max}+1}, P_{i,loss}$	maximum number of retransmissions
λ_i	SNR loss coefficient for NC-QAM
$PER_{i,n}(\gamma_i)$	packet error ratios
$a_{i,n}, g_{i,n}, \gamma_{i,pn}$	parameters of the AM mode n
$\mathcal{R}_{i,n} = \left[\lambda_i^{-1}\gamma_{i,n}, \lambda_i^{-1}\gamma_{i,n+1}\right)$	boundaries of the AM modes for the pair of links
$R_{1,2}, R'_{1,2}, R''_{1,2}$	the instantaneous transmit rate
$\bar{S}_{PSK}, \bar{S}_{PSK}$	bandwidth efficieny

I. INTRODUCTION

The number of mobile users supported by wireless communication networks has increased dramatically, resulting in a booming market for the mobile Internet. Thus there is a growing interest in simultaneous throughput improvements and QoS enhancements. High-rise buildings constitute typical business venues, where cooperative relaying communication is capable of improving the network's coverage and reliability, as shown in Fig. 1. Two-way relaying (TWR), also known as bi-directional relaying, holds the potential of providing practical solutions for enhancing both the spectral efficiency and the reliability for existing wireless networks. Both AF-TWR and DF-TWR constitute popular relaying methods. An example of the AF-TWR or DF-TWR topology is shown in Fig. 1, where two users want to exchange their information using two/three-time-slot protocols. The broadcast nature of bi-directional relaying readily supports the application of network coding in relaying networks.

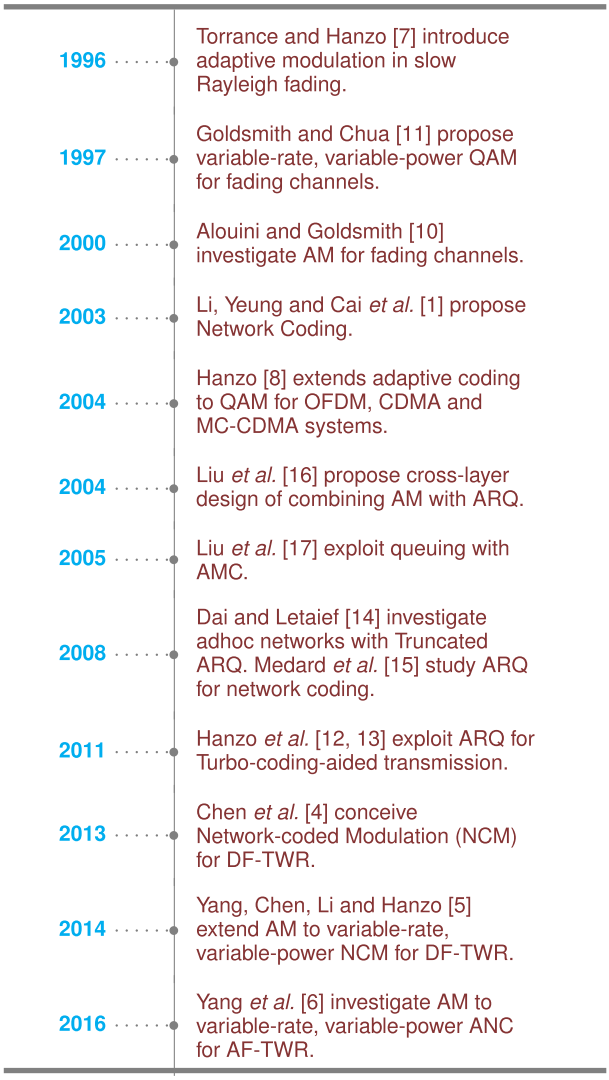

Network Coding (NC) has emerged as a powerful relaying solution owing to its potential of achieving substantial throughput gains [1]–[4]. The landmark contribution of Li *et al.* [1] put forward the linear NC concept for single-source multicast networks, demonstrating that linear codes are capable of approaching the maximum capacity bounds. To the best of our knowledge, [2] was the first NC contribution on the practical subject of simultaneous information exchange between two unicast flows (bi-directional/duplex relaying). Asymmetric transmission problems of TWR were investigated in [3]–[6], separately. Xie [3] investigated the DL capacity of asymmetric DF-TWR. As a further discovery, the authors of [4] and [5] proposed set-partitioning-based NCM as a universal concept, which can be combined with arbitrary constellations. Specifically, our previous work [5], [6] conceived adaptive ANC and NCM based on modulo addition of the normalised phase/amplitude, which circumvented the asymmetric transmission problems of AF- and DF-TWR.

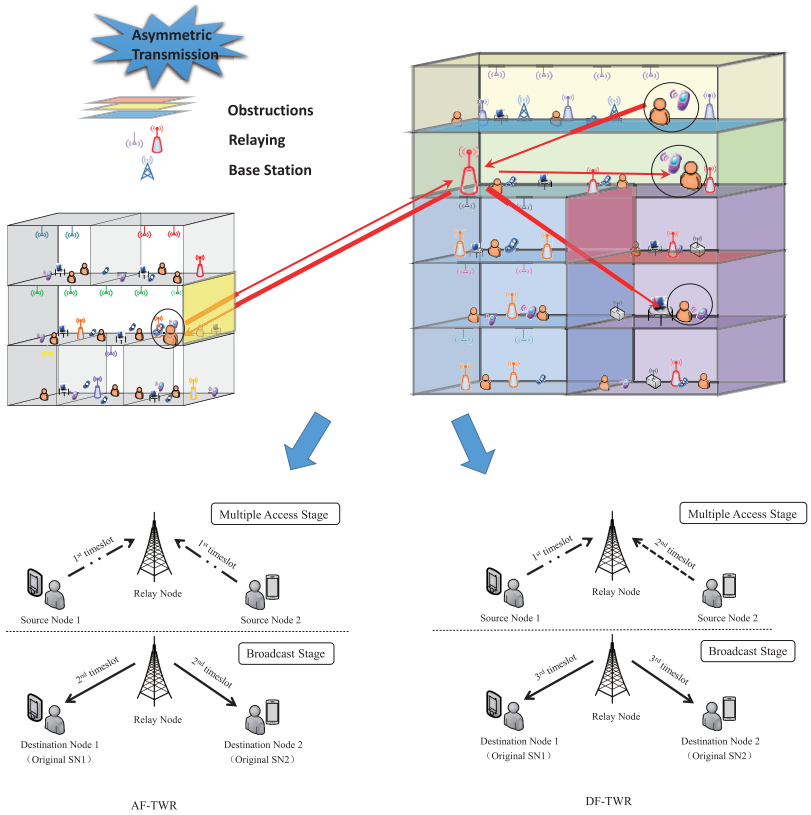

FIGURE 1. Relaying-aided Cooperative Communication for Dense Coverage Network (AF-TWR and DF-TWR scenarios).

However, how to improve both the reliability and throughput of adaptive ANC/NCM communicating over fading channels was left for later study.

In addition to the beneficial throughput improvement of NC-aided relaying, the integrity of data transmission should also be taken into consideration, especially for transmission over fading channels. As one of the key techniques capable of enhancing both the reliability and the throughput for transmission over fading channels, adaptive modulation has received substantial attention [7]–[11]. Hanzo *et al.* designed diverse near-instantaneously adaptive modulation and coding (AMC) techniques in [7], with adaptive coded modulation investigated in [8]–[10]. Alouini and Goldsmith [10] and Goldsmith and Chua [11] conceived adaptive modulation schemes for flat-fading channels, where both the data rate and the transmitter power were near-instantaneously adapted for the sake of maximizing the throughput.

Another alternative technique of achieving high reliability for networks is to rely on the ARQ protocol at the data link layer [12]–[17]. Previous Hybrid ARQ (HARQ) designs were proposed in [12], while AF and DF relaying based on HARQ was studied in [13]. Moreover, adhoc networks relying on ARQ achieving cooperative diversity were presented in [14], while a 'drop-when-seen' algorithm-based ARQ protocol derived for NC was proposed in [15]. Diverse cross-layer designs were investigated in [16] and [17]. Specifically, Liu *et al.* [16], [17] put forward an innovative scheme for conveying delay-sensitive traffic, which combined AMC with the classic truncated ARQ protocol. The proposed scheme improved the attainable throughput, while fulfilling both the associated packet-loss and delay constraints. The underlying core idea behind Liu's cross-layer design [16] is to strike a tradeoff between a reduced physical layer PER and a higher transmission rate. Therefore, by jointly optimizing both the AMC and the truncated ARQ modules, it becomes possible to improve the overall throughput of the system. However, [16] considered a peer-to-peer scenario, and - to the best of our knowledge - truncated-ARQ has not been considered in conjunction with AMC in AF/DF-TWR scenarios in the open literature.

Inspired by the above-mentioned techniques, we conceive a beneficial cross-layer design, which combines adaptive ANC/NCM with NC-based truncated ARQ protocols for the pair of links in AF/DF-TWR networks. The first challenge is to select a meritorious retransmission protocol, which strikes a compelling throughput versus complexity trade-off. A pair of practical NC-based ARQ protocols can be designed based on either the stop-and-wait ARQ (SW-ARQ) or on the selective-repeat ARQ (SR-ARQ). The second challenge is to minimize both the associated delays and buffer sizes.

Hence we consider truncated ARQ protocols for limiting the maximum number of retransmissions. Finally, we characterize the PER vs SNR characteristics of AMC with the aid of a curve-fitting method based on the approach of [16]. More explicitly, we have to design a new transmission strategy for the specific ARQ-aided NC-QAM in order to mitigate the SNR-loss associated with the different transmit rates for the DL of DF-TWR. In conclusion, we have to design a hitherto unexplored solution, which is a qualitatively evolved, intrinsically amalgamated new regime. The proposed regime improves the achievable throughput of AF/DF-TWR networks.

Against the above rationale and the inspirational contributions of [5], [6], and [16], we list the main contribution of this paper as follows.

1) We intrinsically amalgamate the adaptive ANC/NCM techniques of [5] and [6], the truncated-ARQ technique of [16] and the Adaptive Modulation (AM) technique of [10]. The amalgamated design is conceptually complex but powerful. We emphasize that this system is not a simple conglomerate of its components, but it is based on a conscious step-by-step joint design.
2) We extend the peer-to-peer transmission regime of [16] to AF- and DF-TWR networks, where the transmission strategy at the relay node has to simultaneously adapt to a pair of channel conditions, (i.e. SN1→RN→DN2 and SN2→RN→DN1).
3) We design a pair of NC-based ARQ protocols for supporting the proposed transmission strategy.
4) We optimize the transmission rate and analyze the SNR-loss imposed by NC-QAM for DF-TWR network. Then a novel realtime transmission strategy is conceived. We further evaluate the performance of the proposed scheme through extensive simulations. It is shown that the proposed ARQ-aided rate adaptation schemes are superior to their counterparts operating without ARQ, resulting in SNR gains range from 1-3 dB.

This paper tackles the above-mentioned challenges and it is structured as follows. Section II describes both our system as well as channel model adopted, and introduces the proposed cross-layer design. In Section III, a pair of NC-aided protocols are designed for AF/DF-TWR. In Sections IV and V, we introduce the adaptive ANC and NCM scheme followed by the AM regime intrinsically amalgamated with truncated-ARQ retransmission, where a novel transmission strategy is conceived for DF-TWR. Finally, we evaluate the achievable throughput and present our numerical results in Section VI. Our concluding remarks are provided in Section VI.

II. PRELIMINARIES AND ASSUMPTIONS

A. SYSTEM AND CHANNEL MODEL

Consider the AF/DF-TWR networks associated with a multi-carrier TDM/TDMA system, which employs time division duplexing (TDD). Fig. 1 describes a two time-slot AF-TWR and a three time-slot DF-TWR network consisting of a relay node (RN) and two destination nodes (DN1 and DN2),[1] which want to exchange their messages through the RN utilizing the classic time-division technique. The information exchange between the two nodes can be divided into two distinct phases: the multiple access (MA) stage when the two SNs simultaneously/separately send their data to the RN,[2] and the broadcast (BC) stage, when the RN broadcasts the combined signal to both DNs.

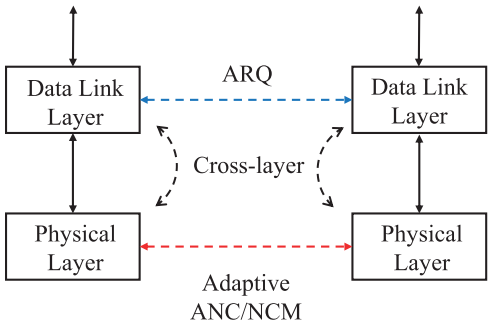

FIGURE 2. Cross-layer Structure Combining NCM with ARQ ([16, Fig. 2]).

Proceeding now with the AF/DF-TWR description of the cross-layer framework, as is shown in Fig. 2, which relies on the ANC/NCM aided AF/DF-TWR of [5] and [6] at the physical layer, and on the truncated ARQ assisted AM regime advocated in [16]. We then conceive an amalgamated adaptive NC scheme combined with truncated ARQ. Fig. 3 shows our particular system and channel model, which consists of the ANC/NCM transmitters, two receivers, two feedback loops required for supporting our adaptive NC and ARQ, two Nakagami fading channels, and buffer modules necessary for the ARQ protocol. For flat fading channels, we adopt the general Nakagami-m model having the fading distribution $p(\gamma_i)$ given by

$$p(\gamma_i) = \frac{m^m \gamma_i^{m-1}}{\overline{\gamma_i}^m \Gamma(m)} \exp\left(-\frac{m\gamma_i}{\overline{\gamma_i}}\right), \quad i = 1, 2, \qquad (1)$$

where γ_i represents the instantaneous SNR, $\overline{\gamma}_i$ denotes the average SNR, $\Gamma(m) := \int_0^\infty t^{m-1} e^{-t} dt$ is the Gamma function and m is the Nakagami fading parameter. The Nakagami distribution can model wide-ranging fading conditions spanning from Rayleigh fading to the friendliest AWGN channel.

Based on the channel model of Fig. 3, the detailed information flow within this framework will be clarified next.

B. INFORMATION FLOW OF AF/DF RELAYING NETWORK

At the physical layer, multiple transmission modes are available. Bearing in mind that the channels are reciprocal, the circularly symmetric complex Gaussian channel gains of the AF links SN1→RN→DN2 and SN2→RN→DN1 are denoted by g_{1r}, g_{r1}, g_{2r} and g_{r2}. For flat fading channels, the channel gains remain the same for some time, hence we

[1] DN1 and DN2 also act as Source node 1 (SN1) and SN2 during the multiple access stage.

[2] For DF-TWR, the two SNs transmit in two different time slots to avoid the mutual interference [4].

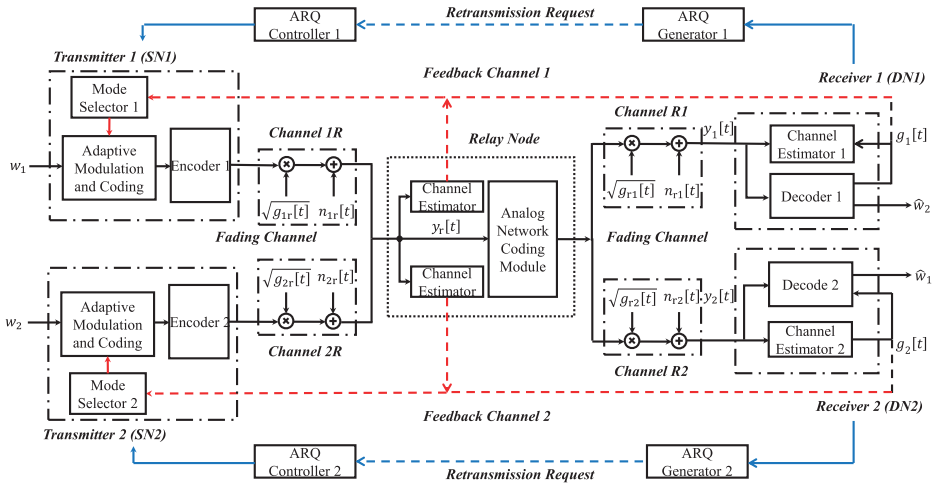

a)

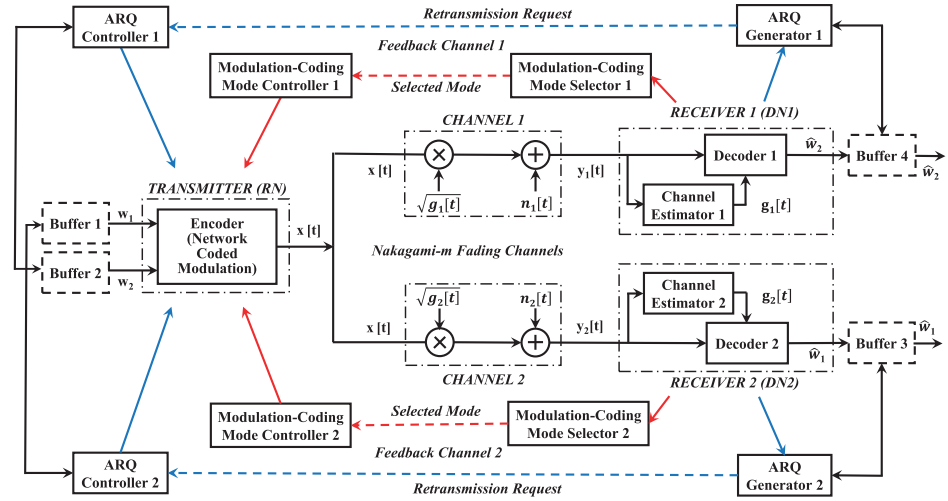

b)

FIGURE 3. System and Channel Models of Adaptive ANC/NCM with ARQ for AF/DF-TWR. a) System and Channel Model of Adaptive ANC (AF-TWR). b) System and Channel Model of Adaptive NCM (Downlink of DF-TWR).

assume $g_{1r} = g_{r1}$ and $g_{2r} = g_{r2}$. For convenience, we denote them as g_1 and g_2. For the DF links RN→DN1 and RN→DN2,[3] we again denote the channel gains as g_1 and g_2. Moreover, the AWGN terms of all links are assumed to have a zero-mean and an equal variance of N_0.

As for our adaptive transmission regime designed for flat fading channels in Fig. 3, we consider a discrete-time channel having a stationary and ergodic time-varying gain $\sqrt{g_i[t]}$ and AWGN $n_i[t]$, with t denoting the discrete time instants. It is assumed that the system uses ideal Nyquist data pulses having a bandwidth of $B = 1/T_s$, where T_s denotes the symbol duration. The instantaneous received SNRs are $\gamma_i[t] = \overline{P} g_i[t]/(N_{0_i} B)$, while the average received SNRs are $\overline{\gamma_i} = \overline{P}/(N_{0_i} B)$, with P denoting the transmit power. When the context is unambiguous, we will omit the time reference t related to g_i and γ_i.

Having outlined the symbols adopted in Fig. 3, the information flow of AF/DF relaying can be characterized as follows. For AF-TWR, the superposed signal received at RN is:

$$y_r^{SN1\to RN} = \sqrt{P_1} h_1 x_1 + \sqrt{P_2} h_2 x_2 + z_{nr}. \quad (2)$$

DN1 and DN2 recover their intended messages by subtracting the message of their own, and get:

$$y_1^{RN\to DN1} = h_1 \alpha \sqrt{P_2} h_2 x_2 + h_1 \alpha z_{nr} + z_{n1}, \quad (3)$$
$$y_2^{RN\to DN2} = h_2 \alpha \sqrt{P_1} h_1 x_1 + h_2 \alpha z_{nr} + z_{n2}, \quad (4)$$

with α is the amplification factor.

[3]Messages in the RN of DF-TWR are decoded and processed, therefore we only consider the RN-DNs DL design. In this case it is assumed that the RN has successfully received the signals w_1 and w_2 from both SN1 and SN2 during the MA stage.

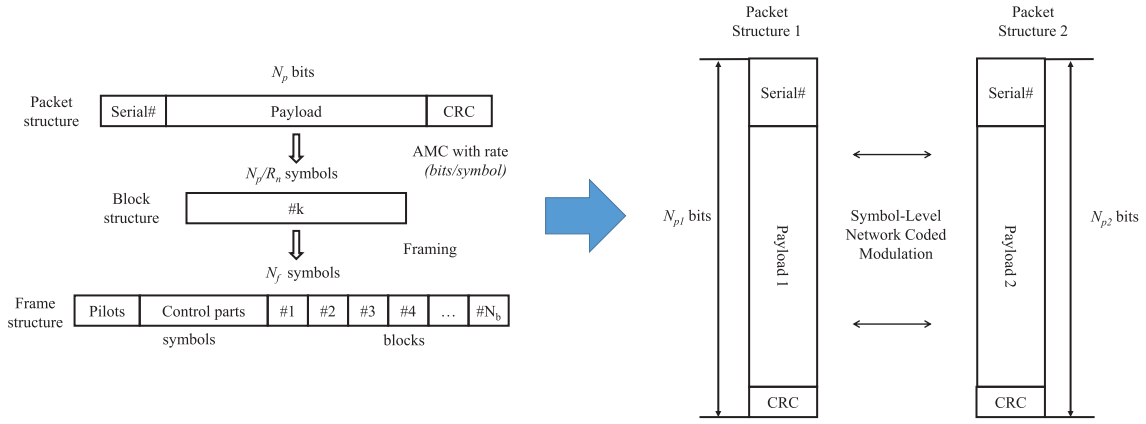

FIGURE 4. Packet and Frame Structures (based on [16, Fig. 3]) and Foundation of NC-aided Protocols (Subsection IV A).

For downlink of DF-TWR, the equivalent baseband signals received by the coherent receiver of DN1 and DN2 are represented by:

$$y_i = h_i x + z_i, \quad i = 1, 2, \tag{5}$$

where x denotes the transmit symbol at the RN, where NCM regime based on the modulo addition of the normalised phase/amplitude is invoked. The generation algorithms of the NC-QAM/PSK symbols are the same as [4]. After both DNs receive the signals, the classic maximum a posteriori probability (MAP) detection rule is applied at both DN's receivers. The specific receiver design for DF relay is available in [4].

Both adaptive ANC and NCM are designed based on the above signal flow. The underlying core idea behind AM is to activate the highest-throughput transmit-mode, which is capable of 'just' meeting the BER requirements. Both the ANC and NCM designs adopt BER bounds to approximate the theoretical BER expressions [18]. This allows us to apply the data-link layer's ARQ technique to TWR, because ANC/NCM has the same BER performance as that of traditional AM. Explicitly, in truncated-ARQ aided AM scheme of [16], the transmit rate is appropriately adjusted, depending on the near-instantaneous SNR γ_i. When the receiver side SNRs obey $\gamma_i \in \mathcal{R}\left[\gamma_{i,n}, \gamma_{i,n+1}\right), n = 0, 1, \ldots, N_i$, we choose the corresponding constellation sizes M_i.

Given this transmission description and based on both AM and ARQ techniques, we will briefly summarize the assumptions adopted throughout this paper.

- The relay node is assumed to operate in the conventional half-duplex mode, relying on an adaptive design at the SNs/RN.
- Frequency-flat, slowly-varying fading channels are assumed, where the channel quality is constant during each transmission-frame but fluctuates from frame to frame. Thus our AM scheme may be reconfigured on a frame-by-frame basis.
- The channel state information (CSI) is perfectly known at all nodes. The perfect CSI-feedback conditions may be approached by using training-based channel estimation.
- Sufficiently reliable CRC codes are used.[4]

C. CROSS LAYER STRUCTURE

Observe in Fig. 3 that our cross layer designs relies on AM at the physical layer, and truncated ARQ at the data link layer. To elaborate a little further, our AM scheme relies on two pairs of control groups. Each pair contains an ARQ control feedback loop and an AM mode feedback loop. The related parameters of each pair of loops are sent back via the same physical feedback channel. Truncated ARQ protocols are implemented based on the NC design, which will be detailed in Section III. More explicitly, buffering modules of Fig. 3 are specialized for the NC-aided SR-ARQ. The ARQ generators and controllers arrange for the retransmission of the requested information stored in the buffers 1-4.

Fig. 4 describes the data structure of the cross-layer design. The processing unit at the data link layer is constituted by a transmission packet, while that of the physical layer is a transmission frame [16], where each frame contains N_f number of symbols. More explicitly, each frame contains multiple packets, where each packet contains N_p bits, which includes both the serial number, as well as the payload and the cyclic redundancy check (CRC)[5] bits to facilitate error detection. When the transmit rate R_n is selected for mode n, each packet is mapped to a symbol-block containing N_p/R_n symbols. Multiple such blocks, together with the N_c pilot symbols and the control messages, constitute a frame to be transmitted at the physical layer.

The key point for the intrinsic amalgamation of AM and ARQ lies in the packet structure, where the packet's data will be mapped into symbols. We can therefore employ symbol-level NC process, which is the foundation of ANC/NCM

[4]Specifically, the serial number and the CRC parity bits of each packet are excluded from the throughput calculation, because they introduce negligible redundancy in addition to the number of payload bits.

[5]The error detection CRC codes uses CRC-24bit check, as standard in [21].

for AF/DF-TWR. Of particular note is that the payload lengths contained in a single packet of the different links are variable, which is necessary for producing the same number of information symbols. Then this constraint guarantees that both the frames generated for the pair of links have the same number of symbols for ensuring the NC operation. There is no similarly strict requirement for AF-TWR, because the messages at the relay are directly superimposed.

III. NC-AIDED ARQ PROTOCOLS DESIGN

Having outlined the cross-layer structure, we next proceed with the design of ARQ protocols. Traditional ARQ protocols mainly include stop-and-wait (SW)-, go-back-N (GBN)-, selective repeat (SR)- and hybrid-ARQ. The choice of the ARQ protocol depends on the application scenario considered. When we design ARQ protocols for ANC/NCM, it is important to take into account the tradeoff between the system's throughput, latency, energy and design complexity. We aim at selecting applicable protocols, which have little or no effect on ANC/NCM. For this reason, two kind of ARQ protocols are considered, namely NC-based SW-ARQ and NC-based SR-ARQ.

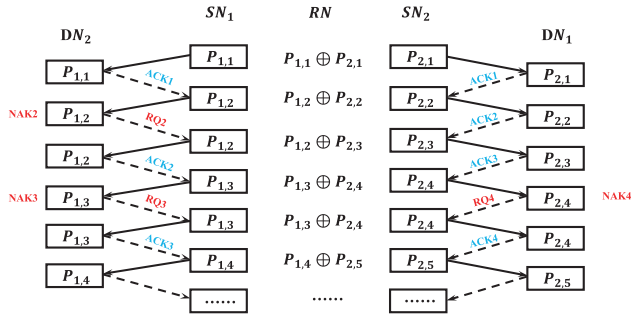

FIGURE 5. NC-based SW-ARQ for ANC/NCM.

A. NC-BASED SW-ARQ PROTOCOL

The basic idea of SW-ARQ is to ensure that each packet has been received correctly, before initiating the transmission of the next packet. Fig. 5 describes the NC-based SW-ARQ transmission process. Let $P_{1,k}$, $k = 1, 2, \ldots$ and $P_{2,k}$, $k = 1, 2, \ldots$ represent the packets transmitted from SN1 to DN2 and from SN2 to DN1, respectively. Each pair of $P_{1,k}$ and $P_{2,k}$ will be merged into a single packet by their modulo two addition at the RN. Then the resultant merged packet will be broadcast to both DN1 and DN2. The first packet received at the RN is transmitted in the first frame and then the transmissions are paused. If the packets demodulated at both DNs are error-free, DN1 and DN2 send an acknowledgement (ACK) back to SN2 and SN1, respectively. In designing this ARQ protocols, the feedback signals are transmitted from DN1 to SN2 through RN and vice versa. If the packet demodulated at any of the DNs is a corrupted packet, say, at DN2, then DN2 sends a negative acknowledgment (NAK) or Retransmission reQuest (RQ) signal back to SN1 via RN. Hence SN1 retransmits the packet required.

There are two advantages of the NC-based SW-ARQ protocol. Firstly, when one of the receptions is corrupted, the other side can operate normally without the need for retransmission. Secondly, there is no need for buffering modules for this protocol, therefore the design complexity is reduced. The primary disadvantage of this protocol is that it provides a relatively low throughput owing to pausing its transmissions.

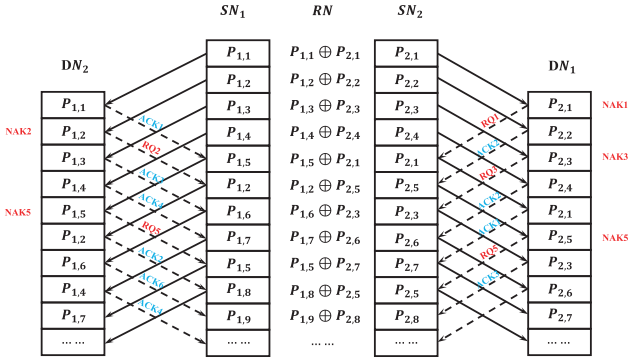

FIGURE 6. NC-based SR-ARQ for ANC/NCM.

B. NC-BASED SR-ARQ PROTOCOL

If we allow for buffering at both the RN and the DNs (only DNs for AF-TWR), we can implement our NC-based SR-ARQ protocol, as shown in Fig. 6. When adopting our NC-based SR-ARQ, there is no need for waiting, therefore it constitutes a continuous-mode transmission protocol. In this design, the transmit packets and decoded packets will be stored in buffers 1-4 seen in Fig. 2. The RN sends a continuous stream of merged packets. If there are any retransmission requests, take DF-TWR for example, owing to an NAK signal for $P_{2,3}$ at DN1, the RQ signal will be sent to the RN. Then the RN adjusts its pointer in buffer 2 to return to the specific point at which it stopped and resumes the transmission of new packets. In this case, each retransmission request results in the retransmission of a single packet.

As a benefit, NC-based SR-ARQ has a higher throughput than NC-based SW-ARQ, albeit its design complexity is also increased.

IV. COMBINING ANALOG NETWORK CODING WITH TRUNCATED-ARQ FOR AF-TWR

In cooperative relying networks, the simplest relaying technique is constituted by the amplify forward protocol. In AF relaying, the relay amplifies the message received from the source node and simply broadcasts the superposed signal to the terminals. Let us first consider the amalgamation of ARQ with physical-layer adaptive ANC.

As stated in Section II, our ANC scheme relies on the BER bounds of [6], which guarantees the same performance as the traditional AM scheme. Traditional AM combined with ARQ was designed based on the relationship of the BER and PER. Let us now discuss our adaptive ANC design. Two groups of transmission modes can be developed, namely the

convolutionally coded M_n-ary QAM/PSK modes[6] and the uncoded M_n-ary QAM/PSK modes. For the former transmission modes, there are no closed-form expressions for PER and BER. We may hence obtain both PER and BER expressions by Monte Carlo simulations. By contrast, for the uncoded latter modes, the closed-form PER expressions of QAM have already been derived in (cf. [20, eqs. (21)–(23)]). We found that for uncoded QAM, upon substituting [20, Eq. (22)] into [16, eq. (20)], the same PER results can be obtained. Therefore we have unified the PER expressions for ANC-QAM/PSK as

$$PER_i = 1 - (1 - BER_i)^{N_{p_i}}, \quad i = 1, 2, \tag{6}$$

where N_{p_i} is the number of bits contained in a packet for the different links.

From a BER performance perspective, the pair of links could also be equivalently viewed as two independent links, as illustrated in Fig. 3 a). Therefore the peer-to-peer AM combined with ARQ [16] may be directly applied to ANC for an AF-TWR scenario. Having designed the ANC-ARQ framework, we next provide a performance analysis of adaptive ANC combined with Truncated-ARQ. From the above analysis and Eq. (6) it can be concluded that our ANC combined with truncated-ARQ is capable of attaining the same throughput as the traditional ARQ-aided scheme, whilst our new scheme supports the more complicated bi-directional scenario. Finally, we should mention that the retransmission design of each AF link is the same as in calssic peer-to-peer ARQ design, and it is partially similar to the ARQ design that will be detailed next.

V. COMBINING ADAPTIVE NC-QAM/PSK WITH TRUNCATED ARQ FOR DF-TWR

This section deals with our cross-layer design conceived for the downlink of DF-TWR. We firstly reformulate the constraints by carefully customizing them for the cross-layer design of DF-TWR. Then in Subsection A we investigate our adaptive NC-QAM/PSK scheme relying on our PER expressions and on the fading region division philosophy of [5]. In Subsection B, based on our designs, a novel transmission mechanism is proposed for determining what specific transmit rates should be adopted for maximizing the average throughput in real-time systems, whilst satisfying the PER and delay constraints. Subsection C details our performance analysis.

According to the particular constraints of ARQ detailed in [16], only finite delays and buffer sizes can be afforded for practical reasons. Additionally, to conceive the truncated-ARQ aided adaptive NCM advocated, we have to carefully consider the intriguing character of NC-QAM. In summary, we formulate the constraints in pairwise form as follows:

- NC-QAM suffers from a modest SNR-loss due to the direct current (DC) bias of two-way communications.[7]

[6]Coded QAM is adopted from the HIPERLAN/2 or IEEE 802.11a standards [21], which is also adopted in [16].

[7]The derivation of SNR-loss is provided in [5].

TABLE 1. SNR-loss coefficients of uncoded NC-QAM.

	4QAM$\|M_1$	16QAM$\|M_1$	64QAM$\|M_1$
4QAM$\|M_2$	$\lambda_1=1, \lambda_2=1$	$\lambda_1=1, \lambda_2=\frac{4}{5}$	$\lambda_1=1, \lambda_2=\frac{16}{21}$
16QAM$\|M_2$	$\lambda_1=\frac{4}{5}, \lambda_2=1$	$\lambda_1=1, \lambda_2=1$	$\lambda_1=1, \lambda_2=\frac{20}{21}$
64QAM$\|M_2$	$\lambda_1=\frac{16}{21}, \lambda_2=1$	$\lambda_1=\frac{20}{21}, \lambda_2=1$	$\lambda_1=1, \lambda_2=1$

This pair of coefficient is given by

$$\lambda_i = \begin{cases} \dfrac{1-{M_i}^{-1}}{1-{M_1}^{-1}}, & \text{if } M_1 \geq M_2 \geq 2, \quad i=1,2 \\ \dfrac{1-{M_i}^{-1}}{1-{M_2}^{-1}}, & \text{if } M_2 \geq M_1 \geq 2, \quad i=1,2, \end{cases} \tag{7}$$

with M_1 and M_2 denoting the constellation sizes of the RN→DN1 link and the RN→DN2 link, respectively. As an example, we detail the SNR-loss values of {4, 16, 64} QAM in Table 1.

- Based on [16], $N_{\gamma_i}^{\max}$ is defined as the maximum number of retransmissions, which can be specified upon dividing the maximum tolerable system delay by the round trip delay required for each retransmission.[8]
- In [16], Liu *et al.* quantified the probability of packet loss after $N_{\gamma_i}^{\max}$ retransmissions, which has to be no higher than $P_{i,loss}$. Let us constrain the instantaneous PERs of each downlink to be no higher than $P_{i,0}^{N_{\gamma_i}^{\max}}$. Then we have:

$$\begin{cases} P_{1,0}^{N_{\gamma_1}^{\max}+1} \leq P_{1,loss} \\ P_{2,0}^{N_{\gamma_2}^{\max}+1} \leq P_{2,loss}. \end{cases} \tag{8}$$

More explicitly, by calculating the inverse of Eq. (7) we obtain:

$$\begin{cases} P_{1,0} \leq P_{1,loss}^{\left(\frac{1}{N_{\gamma_1}^{\max}+1}\right)} := P_{1,target} \\ P_{2,0} \leq P_{2,loss}^{\left(\frac{1}{N_{\gamma_2}^{\max}+1}\right)} := P_{2,target}, \end{cases} \tag{9}$$

where $P_{i,target}$ is defined as the target PER constraint for the RN→DN1 and RN→DN2 links, respectively. If a packet is received incorrectly after $(N_{\gamma_i}^{\max}+1)$ retransmissions, we will drop it.

A. ADAPTIVE NCM AMALGAMATED WITH TRUNCATED-ARQ RETRANSMISSION

Let us next consider the amalgamation of ARQ protocols with adaptive NCM. If we invoke AM to satisfy the PER upper-bound of Eq. (11) at the physical layer and employ $N_{\gamma_i}^{\max}$-truncated ARQ at each link layer, both the delay constraints and the throughput requirements will be satisfied.

1) ADAPTIVE NCM DESIGN AT THE PHYSICAL LAYER

The adaptive NCM invoked here is different from the previous adaptive NCM of [5], in that the NCM here

[8]For example, when the QoS requires a delay of less than 600 ms and the average round trip delay is 100 ms, then we have to have $N_{\gamma_i}^{\max} \leq 6$.

TABLE 2. Transmission modes and adjustment for *M*-ary NC-QAM.

	Mode 1	Mode 2	Mode 3	Mode 4	Mode 5	Mode 6
Modulation	4QAM	8QAM	16QAM	32QAM	64QAM	128QAM
Rate(bits/sym.)	2	3	4	5	6	7
$a_{i,n}$	111.5424	94.6210	84.7006	74.2778	66.8472	61.2536
$g_{i,n}$	0.5118	0.1709	0.1024	0.03943	0.02441	0.00969
$\gamma_{i,pn}$(dB)	9.6202	14.2669	16.3681	20.3630	22.2833	26.2752
When $M_1 = 32$, we get $M_2 \in \{4, 8, 16\}$, PER parameters with SNR-loss for the RN-DN2 link						
$a'_{2,n}$	111.2646	91.8151	87.4836			
$g'_{2,n}$	0.3969	0.1539	0.09941			
$\gamma'_{2,pn}$(dB)	10.7428	14.6550	16.4780			

TABLE 3. Transmission modes for *M*-ary PSK modulation.

	Mode 1	Mode 2	Mode 3	Mode 4	Mode 5
Modulation	QPSK	8PSK	16PSK	32PSK	64PSK
Rate(bits/sym.)	2	3	4	5	6
$a_{i,n}$	112.7842	77.2068	57.0372	45.6370	38.1076
$g_{i,n}$	1.0244	0.4508	0.1560	0.04918	0.01478
$\gamma_{i,pn}$(dB)	6.7432	9.9998	14.0822	18.8080	23.8686

is based on packet-by-packet NC operation (as shown in Fig. 4). Nonetheless, they have the same SNR-loss imposed by NC-QAM and this common problem is referred to as the fading-region partitioning problem. Both Alouini and Goldsmith [10] and Yang *et al.* [5] conceived their mode-partitioning for adaptive M-ary QAM based on the associated BER bounds. Pursuing a similar approach, Liu *et al.* [16] proposed their partitioning algorithm based on the PER expressions. Similarly, we conceive our partitioning technique for NC-QAM/PSK based on the PER versus SNR curves generated by simulations and then modeled with the aid of curve-fitting.

Remark 1: The PER expression for NC-QAM/PSK is the same as in Eq. (6). Of particularly note is that for our DF-TWR scenario, NCM relies on symbol-level operation. Therefore it requires that Eq. (6) N_{p_1}, N_{p_2} has to guarantee that both the frames generated for the pair of links have the same number of symbols corresponding to the AM constellation sizes of M_1 and M_2.

Remark 2: Proceeding with the adaptive design, another important constraint is that NC-QAM imposes a modest but non-negligible SNR-loss. Explicitly, this SNR-loss occurs when the AM transmit rates of the two links are different, albeit it is only imposed at the lower rate receiver side. The SNR-loss expression is given by Eq. (10), which corresponds to a spacing reduction of the constellation points. As this loss can be equivalent to the change of SNR, the receiver side SNRs can be expressed as $\lambda_i\gamma_i$, $i = 1, 2$. By previous derivation from BER to PER, the corresponding PERs can be derived by substituting BER into Eq. (6). There is still one thing should be concerned, in contrast to NC-QAM, for NC-PSK we may derive the PERs by substituting the theoretical BER expressions of [21, p. 181] into Eq. (6).

The BER expressions obtained by the above method contain either Q-functions or complementary error functions *erfc(x)*, which cannot be readily inverted. Therefore it is difficult to obtain AM region-partitioning parameters as a function of the SNR and PER. In order to implement the AM-mode partitioning algorithm, we pursue a similar approach to that of [16] to obtain the approximate PER curves, which can be expressed as

$$PER_{i,n}(\gamma_i) \approx \begin{cases} 1, & if\ 0 < \gamma_i < \gamma_{i,pn} \\ a_{i,n}\exp\left(-g_{i,n}\lambda_i\gamma_i\right), & if\ \gamma_i \geq \gamma_{i,pn} \end{cases} \quad i = 1, 2, \tag{10}$$

where $a_{i,n}$, $g_{i,n}$ and $r_{i,pn}$ are the parameters of the AM mode n. In our proposed scheme, these parameters can be obtained by fitting the approximate PERs in Eq. (10) to the exact PERs in Eq. (6). Hence we invoke a curve fitting tool (1stOpt) relying on a Particle Swarm Optimization algorithm to obtain $a_{i,n}$, $g_{i,n}$ and $r_{i,pn}$. The curve fitting parameters derived for the uncoded NC-QAM transmission modes are listed in Table 2, while those of NC-PSK are listed in Table 3. By inverting Eq. (10) we arrive at the partition boundaries $\{\gamma_{i,n}\}_{i,n=0}^{N_i+1}$ as

$$\begin{cases} \gamma_{i,0} = 0 \\ \gamma_{i,n} = \dfrac{1}{\lambda_i g_{i,n}} \ln\left(\dfrac{a_{i,n}}{P_{i,target}}\right) \\ \gamma_{i,N_i+1} = +\infty, \end{cases} \tag{11}$$

where $\{i, n\} = 1, 2, \ldots, N_i$, $i = 1, 2$ denote the AM region partitions for the two DLs, while $P_{i,target}$ is given by Eq. (12). Therefore the boundaries of the AM modes for DN1 and DN2 are:

$$\mathcal{R}_{i,n} = \left[\gamma_{i,n}, \gamma_{i,n+1}\right), \tag{12}$$

where $\{i, n\} = 1, 2, \ldots, N_i$, $i = 1, 2$. Specifically, when $\gamma_i \in \left[\gamma_{i,n}, \gamma_{i,n+1}\right)$, AM mode n is selected.

Note that for NCM, a special case should be considered. For example, the SNR γ_1 obeys $\gamma_{1,0} < \gamma_1 < \gamma_{1,1}$, while we have $\gamma_2 > \gamma_{2,1}$, because in this case no payload bits will be transmitted over the RN→DN1 link. Therefore, we set the packets' bits to 0 for modulo addition so as to ensure the continuity of NCM transmission.

B. STRATEGY OF SELECTING CONSTELLATIONS FOR ADAPTIVE NC-QAM

The corresponding transmission strategy conceived for adaptive NC-QAM adapts the AM modes to the instantaneous SNRs γ_1 and γ_2. Given γ_1 and γ_2 for the RN→DN1 and RN→DN2 links based on the associated channel estimates, our aim is to find the optimal AM constellation sizes of M_1 and M_2 that adapt to γ_1 and γ_2.

As described in the previous subsection, NC-QAM suffers from an SNR-loss. In view of the fact that the SNR-loss is related to the specific choice of M_1 and M_2, it turns out to be quite an interesting point for us to decide, which particular constellation sizes should be activated. According to our analysis, there are two fundamental facts: 1) we find that once the constellation size for a link is fixed, it will affect the choice of constellation picked for the other link; 2) it is found that serendipitously, there is no SNR-loss for the specific link, which has a larger constellation size and hence would require a higher SNR.

Based on the above discussions, we propose a joint selection strategy for obtaining the optimal M_1^* and M_2^*, which adapt to γ_1 and γ_2. Fig. 7 shows the flow chart of the proposed strategy. For the instantaneous SNRs γ_1 and γ_2, we arrive at the optimal M_1^* and M_2^* by invoking ***Step 1)-Step 5)*** listed below and summarized in **Algorithm 1**. When considering the SNR-loss, we find that there are only three cases: $M_1 = M_2$, $M_1 > M_2$ and $M_1 < M_2$. These three cases correspond to no SNR-loss, SNR-loss in the RN→DN2 link and SNR-loss in the RN-DN1 link, respectively.

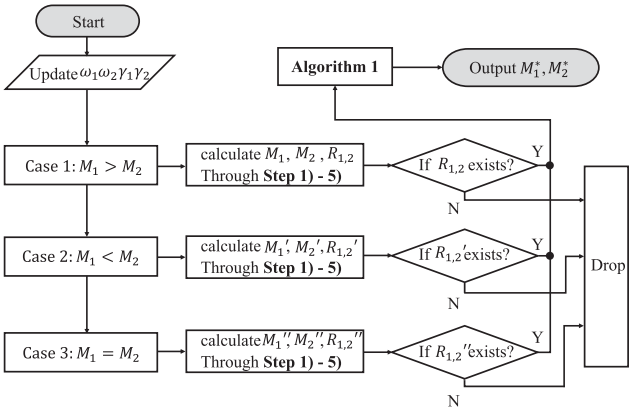

FIGURE 7. Flow chart of selecting M_1^* and M_2^*.

To elaborate further, the transmission strategy is determined by ***Step 1)-Step 5)*** as follows (cf. Fig. 7), where we rely on the weighted average rates for determining the AM mode. The weighting coefficients ω_1 and ω_2 have been introduced for the following reason: if several cases are feasible, for example, $M_1^* = 4$, $M_2^* = 8$ and $M_1^* = 8$, $M_2^* = 4$ are both feasible AM modes, we calculate the weighted average rates according to ω_1 as well as to ω_2, and then decide which mode should be activated. The weights ω_i, $i = 1, 2$ are determined according to the PER-requirement of the RN→DN1 and RN→DN2 links, respectively. Naturally, we have $\omega_1 + \omega_2 = 1$ and $0 \leq \omega_i \leq 1$, $i = 1, 2$.

Step 1): Given the input parameters, such as ω_1, ω_1, γ_1 and γ_2, we firstly determine the AM modes. The constellation sets are set to be $M_1 \in \{4, 8, 16, \ldots 2^{N_1}\}, N_1 = 2, 3, \ldots$ and $M_2 = \{4, 8, 16, \ldots 2^{N_2}\}, N_2 = 2, 3, \ldots$. Secondly, we have to consider the relationship between M_1 and M_2. If $M_1 > M_2$, go to ***Step 2)***; if $M_1 < M_2$, skip to ***Step 3)***; if $M_1 = M_2$, proceed to ***Step 4)***.

Step 2): In this case an SNR-loss exists in the RN-DN2 link. Firstly, we get $\lambda_1 = 1$ and $\lambda_2 = \left(1 - M_2^{-1}/1 - M_1^{-1}\right)$ for the two links according to Eq. (7), respectively, where $\lambda_1 = 1$ implies that there is no SNR-loss in the RN→DN1 link. Therefore we can determine M_1 by substituting γ_1 into Eqs. (12) and Tables 1 and 2. Secondly, we may obtain M_2 according to M_1 under the constraint of $M_1 > M_2$. For example, if $M_1 = 32$, we have $M_2 \in \{4, 8, 16\}$. Then recalculate the rate-region boundaries $\mathcal{R}_{2,n}{}'$ according to λ_2 and Eqs. (10)-(12). Thirdly, if γ_2 falls into the rate-region $\mathcal{R}_{2,n}{}'$, the corresponding M_2 can be selected. Thus we calculate

$$R_{1,2} = \omega_1 \log_2 M_1 + \omega_2 \log_2 M_2, \tag{13}$$

If γ_2 does not fall into $\mathcal{R}_{2,n}{}'$, this case indicates that our assumption is not reasonable, then we drop this case. Finally, go to ***Step 5)***.

Step 3): For the case of $M_1 < M_2$, the SNR-loss exists in the RN→DN1 link, hence we have $\lambda_2 = 1$ and $\lambda_1 = \left(1 - M_1^{-1}/1 - M_2^{-1}\right)$. Using the approach of ***Step 2)***, M_2' and M_1' can be obtained, then we can calculate

$$R'_{1,2} = \omega_1 \log_2 M_1' + \omega_2 \log_2 M_2'. \tag{14}$$

If γ_1 does not fall into $\mathcal{R}_{1,n}{}'$, this case indicates that our assumption is not reasonable. Finally, go to ***Step 5)***.

Step 4): For the case of $M_1 = M_2$, there is no SNR-loss for any of the two DLs. Therefore we may obtain M_1'' and M_2'' for the SN1→DN2 link and the SN2→DN1 link by substituting $\lambda_1 = \lambda_2 = 1$ into Eqs. (10). If $M_1'' = M_2''$, then we calculate

$$R''_{1,2} = \omega_1 \log_2 M_1'' + \omega_2 \log_2 M_2''. \tag{15}$$

If $M_1'' \neq M_2''$, this case indicates that our assumption is not reasonable. Finally, go to ***Step 5)***.

Step 5): One or more above assumptions may be reasonable. Hence we conceive **Algorithm 1** to decide, which particular transmission mode should be activated as the final pair of M_1^* and M_2^*. Finally, the flat fading channels vary from frame to frame, therefore if there are any changes, we have to update γ_1 and γ_2, then go back to ***Step 1)***.

When implementing ***Step 1)-Step 5)*** and **Algorithm 1**, we have to pay attention to the following points. Firstly, for given pair of instantaneous SNRs γ_1 and γ_2, there may be several feasible solutions, but at least one pair of M_1^* and M_2^* exists, which satisfies the PER-target. Secondly, we list a schematic diagram in Table 1,[9] in which we could see apparently the

[9]Table 1 list uncoded modulation cases. Coded modulation cases have similarly values.

Algorithm 1 Constellation Selecting Algorithm

Input: $\widehat{\Re} = \{R_{1,2}, R_{1,2}', R_{1,2}''\}$
Output: M_1^*, M_2^*
Initial: $R_{1,2}$, $R_{1,2}'$ or $R_{1,2}''$
Case 1:
- **If** $R_{1,2} \in \hat{\Re}$, $R_{1,2}' \in \hat{\Re}$ & $R_{1,2}'' \in \hat{\Re}$
  - **If** $R_{1,2} \geq R_{1,2}'$ & $R_{1,2} \geq R_{1,2}''$, let $M_1^* = M_1$ & $M_2^* = M_2$
  - **Elseif** $R_{1,2}' \geq R_{1,2}$ & $R_{1,2}' \geq R_{1,2}''$, let $M_1^* = M_1'$ & $M_2^* = M_2'$
  - **Else** let $M_1^* = M_1''$ & $M_2^* = M_2''$
- **End**

Case 2:
- **If** $R_{1,2} \in \hat{\Re}$, $R_{1,2}' \in \hat{\Re}$ & $R_{1,2}'' \notin \hat{\Re}$
  - **If** $R_{1,2} \geq R_{1,2}'$, let $M_1^* = M_1$ & $M_2^* = M_2$
  - **Else** let $M_1^* = M_1'$ & $M_2^* = M_2'$
- **End**

Case 3:
- **If** $R_{1,2} \in \hat{\Re}$, $R_{1,2}'' \in \hat{\Re}$ & $R_{1,2}' \notin \hat{\Re}$
  - **If** $R_{1,2} \geq R_{1,2}''$, let $M_1^* = M_1$ & $M_2^* = M_2$
  - **Else** let $M_1^* = M_1''$ & $M_2^* = M_2''$
- **End**

Case 4:
- **If** $R_{1,2}' \in \hat{\Re}$, $R_{1,2}'' \in \hat{\Re}$ & $R_{1,2} \notin \hat{\Re}$
  - **If** $R_{1,2}' \geq R_{1,2}''$, let $M_1^* = M_1'$ & $M_2^* = M_2'$
  - **Else** let $M_1^* = M_1''$ & $M_2^* = M_2''$
- **End**

Case 5:
- **If** $R_{1,2} \in \hat{\Re}$, $R_{1,2}' \notin \hat{\Re}$ & $R_{1,2}'' \notin \hat{\Re}$, let $M_1^* = M_1$ & $M_2^* = M_2$
- **Elseif** $R_{1,2}' \in \hat{\Re}$, $R_{1,2}' \notin \hat{\Re}$ & $R_{1,2}'' \notin \hat{\Re}$
  - let $M_1^* = M_1'$ & $M_2^* = M_2'$
- **Else** let $M_1^* = M_1''$ & $M_2^* = M_2''$
- **End**

reason for applying ***Step 2)***-***Step 4)***-that is, there are three cases of SNR-loss, thus they effect the selection of the pair of constellation size. Thirdly, for convenience, we unify some of the parameters in this paper, e.g., the AM mode sets are set to be $M_i \in \{4, 8, 16, \ldots 2^{N_i}\}$, $N_i = 2, 3, \ldots, i = 1, 2$, whilst the delay constraints of the two links are the same. Note that these parameters are variable can be preestablished in practical designs.

To elaborate a little further, as for adaptive NC-PSK with Truncated ARQ design, there is no SNR-loss for the pair of downlinks [5]. Therefore we may simply view the NC-PSK schemes as two independent transmission links. We may thus simply determine the AM modes M_1 and M_2 based on γ_1 and γ_2 by substituting $\lambda_1 = \lambda_2 = 1$ into Eqs. (10)-(12).

C. PERFORMANCE EVALUATION FOR ADAPTIVE NCM WITH TRUNCATED ARQ

The transmission strategy designed in the previous subsection inherently amalgamates AM both with NCM and with ARQ protocols. We evaluate the performance of our truncated-ARQ aided adaptive NCM scheme, relying on the approach of [16].

1) PERFORMANCE OF ARQ-AIDED NC-PSK

For adaptive NC-PSK design, we may view the pair of downlink as two independent downlinks. Therefore we may obtain the overall bandwidth efficiency by calculating

$$\bar{S}_{PSK}\left(N_{\gamma_1,\gamma_2}^{\max}\right) = \omega_1 \bar{S}\left(N_{\gamma_1}^{\max}\right) + \omega_2 \bar{S}\left(N_{\gamma_2}^{\max}\right), \quad (16)$$

where ω_1 and ω_2 are exactly the same as described in the previous subsection. Furthermore, $\bar{S}\left(N_{\gamma_1}^{\max}\right)$ and $\bar{S}\left(N_{\gamma_2}^{\max}\right)$ represent the average bandwidth efficiency, which can be obtained according to Eqs. (21)-(26) in Appendix.

2) PERFORMANCE OF ARQ-AIDED NC-QAM

For adaptive NC-QAM amalgamated with NC-based truncated ARQ, the bandwidth efficiency of this scheme may also be formulated as in Eq. (16). However, the difference between an NC-QAM based and NC-PSK based scheme can be categorized as follows: 1) we cannot view the scheme as two equivalent independent transmissions, because NC-QAM suffers from a modest SNR-loss; 2) we may clearly see that in ***Step 5)*** of previous subsection, there may be several feasible solutions but we take the specific pair of M_1 and M_2 which has the maximum total rate. This however complicates the performance analysis.

The exact bandwidth efficiency is challenging to evaluate, but fortunately we were able to characterize some properties of the SNR-loss. Considering $M_1 > M_2$ for example, the SNR loss of λ_2 is a monotonically increasing function of M_2, but a decreasing function of M_1. Therefore it is lower bounded by (for QAM, $M_i \geq 4$)

$$\lambda_2 = \frac{1 - M_2^{-1}}{1 - M_1^{-1}} > 1 - \frac{1}{M_2} > \frac{3}{4}. \quad (17)$$

Then we may set both an upper bound and a lower bound of the SNR-loss coefficients for NC-QAM combined with truncated ARQ. We set $\lambda_1 = \lambda_2 = 1$ as an upper bound. When we consider the lower bound and assume, for example, $M_1 > M_2$, then it is found that $M_2 \in \{4, 8, 16, 32, 64\}$. Hence for each M_2, we have $\lambda_{2,1} > 3/4$, $\lambda_{2,2} > 7/8, \cdots, \lambda_{2,5} > 63/64$. Let $\lambda_{i,1} = \lambda_{i,2}, \cdots = \lambda_{i,6} = 3/4$, $i = 1, 2$ be the SNR-loss coefficients for both DLs, which allow us to obtain the lower bound. In fact, the bandwidth efficiency is far better than the lower bound due to the fact that we assumed the maximum SNR-loss in both DLs.

Upon setting both the upper bound and lower bound for the SNR-loss, we may view the two downlinks as two independent transmission links. Thus the bandwidth efficiency of NC-QAM can be obtained by the same approach, as for adaptive NC-PSK, yielding:

$$\bar{S}_{QAM}\left(N_{\gamma_1,\gamma_2}^{\max}\right) = \omega_1 \bar{S}\left(N_{\gamma_1}^{\max}\right) + \omega_2 \bar{S}\left(N_{\gamma_2}^{\max}\right), \quad (18)$$

where $\overline{S}\left(N_{\gamma_i}^{\max}\right)$ is given by

$$\overline{S}\left(N_{\gamma_i}^{\max}\right) = \frac{\overline{S}_{e_i,physical}}{\overline{N}\left(p_i, N_{\gamma_i}^{\max}\right)} = \frac{1}{\overline{N}\left(p_i, N_{\gamma_i}^{\max}\right)} \sum_{n=1}^{N_i} R_{i,n} \mathrm{Pr}_i(n), \quad i = 1, 2, \tag{19}$$

where $\overline{S}_{e_i,physical}$, $\overline{N}\left(p_i, N_{\gamma_i}^{\max}\right)$ and $\mathrm{Pr}_i(n)$ can be obtained from Eqs. (21)-(26).

Setting the upper- and lower-bounds for the SNR-loss provides a simple way of analysing the performance of adaptive NC-QAM. Since the SNR-loss tends to decrease upon increasing the constellation sizes, the actual performance may be close to the upper-bound curves according to Table 1.

VI. PERFORMANCE ANALYSIS

The above-mentioned strategy provides the basis for our truncated ARQ aided adaptive ANC/NCM design. In this section, a range of representative numerical results are presented for illustrating and validating our theoretical analysis, relying on bandwidth expressions derived in Section V C and Appendix (cf. Eqs. (10-12), Eqs. (17-19), Eqs. (21-26)). Note that both links of our ANC-ARQ scheme have the same performance as their conventional peer-to-peer counterpart, thus we omit its characterization. Next we unify the simulation parameters as follows.

- *Common Parameter Settings:*
  - Fading distribution: Let the fading channels obey Rayleigh fading. Then the distribution of γ_i is given by letting $m = 1$ in Eq. (1), yielding

$$p(\gamma_i) = \frac{1}{\bar{\gamma}_i} \exp\left(-\frac{\gamma_i}{\bar{\gamma}_i}\right), \quad i = 1, 2. \tag{20}$$

  - Block length: The payload length of a single block should be the least common multiple of $\log_2(M_1)$ and $\log_2(M_2)$. The packet length be $N_{p_i} = 1080$, $i = 1, 2$ symbols for the pair of links.
  - Delay constraints: Let $N_i^{\max} = 3$, $i = 1, 2$ and $P_{i,loss} = 0.01$, $i = 1, 2$.
  - Average SNRs: Let $\overline{\gamma_i} \in [0, 1, \ldots, 30]$, $i = 1, 2$ (dB).
  - Weighting factors: Let $\omega_i = 0.5$, $i = 1, 2$.
  - Bandwidth: let $B = 1$.
  - Both links adopt SR-ARQ protocols.
  - Performance analysis equations: Eqs. (21)-(26) in Appendix.
- *Figure 8 Parameter Settings:*
  - Constellation size for RN→DN1 link: $M_1 = 32$.
  - Constellation sets for RN→DN2 link: $M_2 \in \{4, 8, 16\}$.
  - Adaptive modes: Modes 1, 2 and 3 in Table 2.

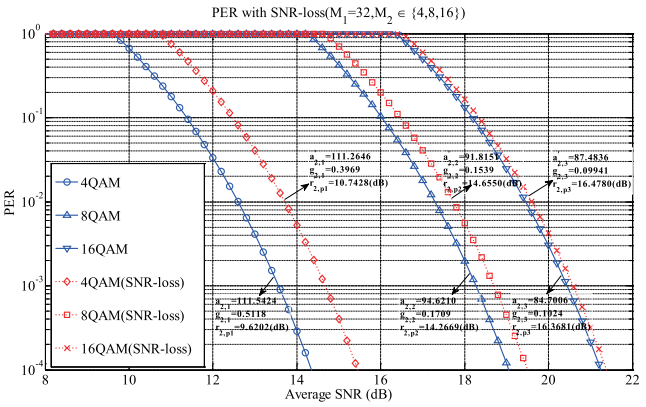

FIGURE 8. PER change along with SNR-loss for RN-DN2 Link (Table 2).

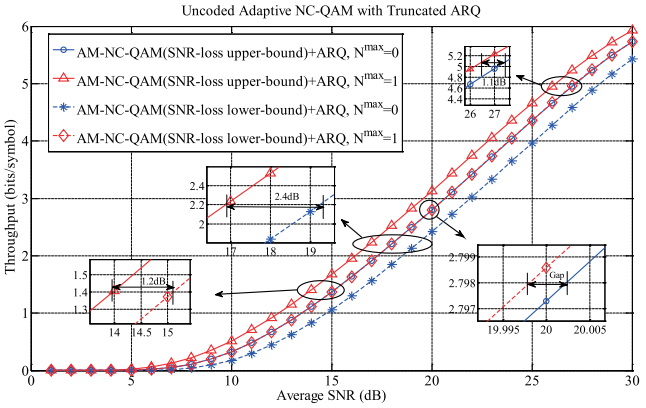

FIGURE 9. Performance of adaptive NC-QAM with NC-based ARQ versus Average SNR.

- *Figure 9 Parameter Settings:*
  - M-ary uncoded NC-QAM[10] adaptive modes: Let $M_i \in \{4, 8, 16, 32, 64, 128\}$.
  - SNR-loss bounds according to Eq. (17): Let $\lambda_i = 1$, $i = 1, 2$ be the upper bound, while $\lambda_i = 3/4$ be the lower bound.
  - The ARQ retransmission index: $N_i^{\max} = 0$, $i = 1, 2$ and $N_i^{\max} = 1$, $i = 1, 2$.
- *Figure 10 Parameter Settings:*
  - M-ary coded NC-QAM adaptive modes: Let $M_i \in \{4, 8, 16, 32, 64\}$.
  - SNR-loss bounds: Let $\lambda_i = 1$, $i = 1, 2$ be the upper bound, while $\lambda_i = 3/4$ be the lower bound.
  - The ARQ retransmission index: $N_i^{\max} = 0$, $i = 1, 2$ and $N_i^{\max} = 1$, $i = 1, 2$.
- *Figure 11 Parameter Settings:*
  - M-ary uncoded NC-QAM adaptive modes: $M_i \in \{4, 8, 16\}$.
  - The ARQ retransmission index: $N_i^{\max} \in \{0, 1, 2, 4, 8\}$, $i = 1, 2$.
- *Figures 12 Parameter Settings:*
  - M-ary uncoded NC-PSK adaptive modes: $M_i \in \{4, 8, 16, 32, 64\}$.

[10]HIPERLAN/2 or IEEE 802.11a standards [21].

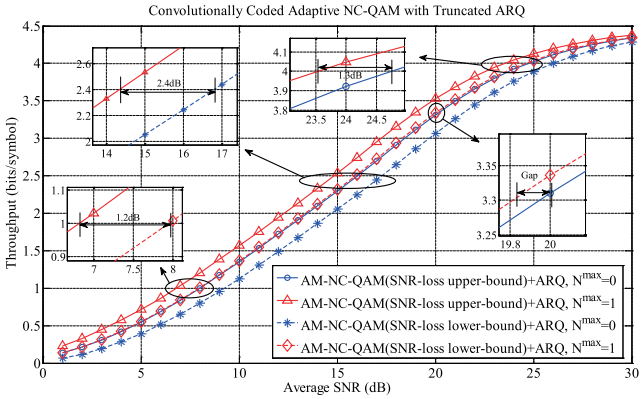

FIGURE 10. **Performance of adaptive NC-QAM with NC-based ARQ versus Average SNR.**

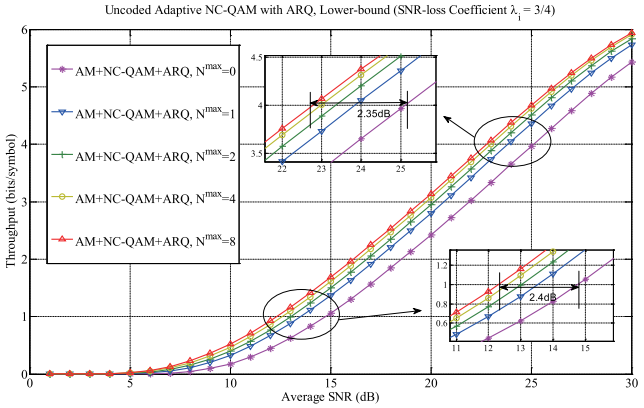

FIGURE 11. **Lower-bound performance of adaptive NC-QAM for DF-TWR.**

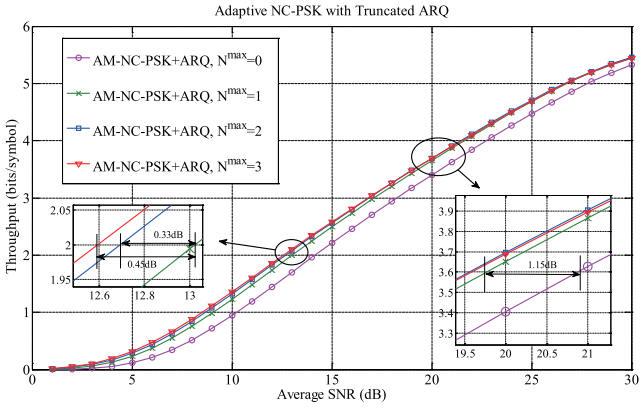

FIGURE 12. **Performance of adaptive NC-PSK with NC-based ARQ for DF-TWR.**

  - The ARQ retransmission index: $N_i^{\max} \in \{0, 1, 2, 3\}$, $i = 1, 2$.

- *Figures 13 Parameter Settings:*
  - M-ary uncoded NC-PSK adaptive modes: $M_i \in \{4, 8, 16, 32, 64\}$.
  - The ARQ retransmission index: $N_i^{\max} \in 1, i = 1, 2$.
  - Nakagami-m fading parameter: $m = 1, 2, 3, 4$.

Of particular note for the parameters of Fig. 8 is that Table 2 lists the PER curve-fitting parameters $a_{i,n}$, $i = 1, 2$, $g_{i,n}$ and $\gamma_{i,pn}$ for NC-QAM. In order to visualize the effects of SNR-loss, we briefly consider a special case of the SNR-loss for $M_1 = 32$ and $M_1 > M_2$. In this case, we have to recalculate the PER-curve fitting parameters for $M_2 \in \{4, 8, 16\}$. The parameters $a'_{2,n}$, $g'_{2,n}$ and $\gamma'_{2,pn}$ are then listed in Table 2.

We plot PER for the scenarios of both with and without SNR-loss for the RN→DN2 link in Fig. 8. Observe that the gaps between the curves with and without SNR-loss tend to become narrow upon reducing the difference between M_1 and M_2. This indicates that the throughput-loss decreases upon increasing M_1 and M_2. It also worth noting that the reduction of the overall throughput is related to the changes between $\gamma_{2,pn}$ and $\gamma'_{2,pn}$ in Table 2. The higher constellation sizes, the smaller integration intervals (compared to the ranges without SNR-loss), which led to the performance degradation (cf. Eq. (17)).

Upon analyzing the effects of SNR-loss and of the proposed transmission strategy, we plot the throughput of both uncoded and convolutionally coded adaptive NC-QAM in conjunction with the maximum number of ARQ retransmissions $N_i^{\max} = 1$, $i = 1, 2$ in Figs. 9 and 10. It can be observed that in all cases, the proposed method is superior to its counterparts operating without ARQ, where the throughput gain ranges from 0.2 to 0.7 bits/symbol. We will offer further observations during our forthcoming discourse.

1) Based on the transmission strategy proposed in Subsection V B, we plot the performance of the schemes, when the SNR-loss coefficients rely either on the upper- or on the lower-bound. Observe that the upper-bound curves exceed the lower-bound curves by about 0.25 bits/symbol, when using only a single retransmission of $N_i^{\max} = 1, i = 1, 2$ for both schemes.
2) Compared to the AM-NC-QAM schemes operating without ARQ, $N_i^{\max} = 1$, $i = 1, 2$ offers about 1 dB SNR gain.
3) For NC-QAM associated with an SNR-loss, at best we are able to obtain an approximately 2.4 dB SNR gain for the special case, when M_1 is equal to M_2. According to our conservative estimates, our proposed AM-NC-QAM associated with $N_i^{\max} = 1, i = 1, 2$ achieved an approximately 1-2 dB gain.

In Fig. 11 we plot the lower bound of throughput for NC-QAM with ARQ. We observe that the throughput improves with the increasing of $N_i^{\max} = 1, 2, 4, 8$, $i = 1, 2$. In the maximum case, we could obtain approximately 2.4 dB gain. However, the increment degrades quickly, which implies that $N_i^{\max}$ need not be arbitrarily large. This is a trade-offs between throughput and delay as well as buffer-size penalties.

In order to complete our adaptive NCM design, we detail the PER-curve-fitting parameters of NC-PSK in Table 3 and characterize the attainable throughput in Fig. 12. We also plot throughput of NC-PSK with ARQ for Nakagami fading

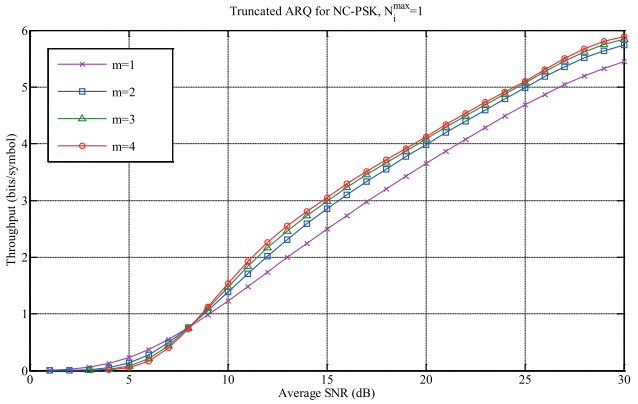

FIGURE 13. Performance of adaptive NC-PSK with ARQ under nakagami-*m* channels.

parameter $m = 1, 2, 3, 4$ in Fig. 13. There are some points worth noting.

1) Observe in Fig. 12 that $N_i^{\max} = 3$, $i = 1, 2$ offers an approximately 1.6 dB SNR gain over the NC-PSK schemes operating without ARQ. We would expect similar conclusions also for NC-QAM.
2) Blindly increasing the number of retransmissions does not always result in further gains, because they improve the reliability of packets at the expense of an increased delay.
3) It is confirm that the throughput gain increases with the diversity order m,[11] which is similar to the case of varying N_i^{max}.
4) Compared to peer-to-peer transmissions, our proposed NC-QAM/PSK regimes support the more challenging scenario of bidirectional NC aided networks. Our holistic design has the advantage of improved adaptability and flexibility.

VII. CONCLUSIONS

In this paper, we developed a powerful cross-layer design for asymmetric AF-TWR and DF-TWR networks, which amalgamates adaptive ANC/NCM at the physical layer and NC-based truncated ARQ at the data link layer, with the objective of improving the attainable system throughput and enhancing the achievable system integrity. We developed a pair of two basic NC-aided ARQ protocols for ANC/NCM for the sake of characterizing the tradeoff between the design complexity and system throughput. Then cross-layer design aided AF and DF relaying was conceived. More explicitly, a joint AM-mode selection strategy was developed for both DF downlinks for the sake of determining the optimal constellation sizes, which are carefully matched to the instantaneous SNRs. Furthermore, we evaluated the average throughput of adaptive ANC/NCM based on the PER-based fitted curves. Specifically, both an upper and a lower bound were derived for the SNR-loss coefficients of NC-QAM. Our performance analysis demonstrated that the proposed adaptive ANC/NCM relying on NC-aided ARQ is capable of achieving a higher throughput than its counterparts operating without retransmissions.

Our cross-layer design is capable of supporting practical applications, such as 5G ultra-dense cellular networks [22], sensor networks and satellite communications. As to future research, it is possible to extend ANC/NCM for combining it with existing physical layer techniques, such as channel coding [23] and MIMO [24]. Another possible extension of this work is to develop and analyze an NC-based H-ARQ protocol for retransmission design. Finally, latency performance and trade-off analysis of the proposed method, as well as the specific impact of data link layer on physical layers are also worth characterizing, which will be left for future work.

[11] The Nakagami-*m* fading channel provides a diversity order of *m*, which means Nakagami-*m* fading channel is equivalent to a set of *m* independent Rayleigh fading channels by adopting maximum ratio combining (MRC).

APPENDIX

For convenience, here we only list the equations used in Section V C without further detailed explanations, which refer to [16]:

$$\bar{S}_{e,physical} = \sum_{n=1}^{N} R_n \Pr(n), \tag{21}$$

$$\Pr(n) = \int_{\gamma_n}^{\gamma_{n+1}} p_\gamma(\gamma)\, d\gamma = \frac{\Gamma\left(m, \frac{m\gamma_n}{\bar{\gamma}}\right) - \Gamma\left(m, \frac{m\gamma_{n+1}}{\bar{\gamma}}\right)}{\Gamma(m)}, \tag{22}$$

$$\Gamma(m) := \int_0^\infty t^{m-1} e^{-t} dt, \tag{23}$$

$$\bar{N}\left(p, N_\gamma^{\max}\right) = 1 + p + p^2 + \ldots + p^{N_\gamma^{\max}} = \frac{1 - p^{N_\gamma^{\max}+1}}{1-p}, \tag{24}$$

$$p := \overline{PER} = \frac{\sum_{n=1}^{N} R_n \Pr(n)\, \overline{PER}_n}{\sum_{n=1}^{N} R_n \Pr(n)}, \tag{25}$$

$$\overline{PER}_n = \frac{1}{\Pr(n)} \frac{a_n}{\Gamma(m)} \left(\frac{m}{\bar{\gamma}}\right)^m \times \frac{\Gamma(m, b_n\gamma_n) - \Gamma(m, b_n\gamma_{n+1})}{(b_n)^m}, \tag{26}$$

with b_n is the function of g_n and $\bar{\gamma}$. Specifically, let $m = 1$ for Rayleigh fading channel.

REFERENCES

[1] S.-Y. R. Li, R. W. Yeung, and N. Cai, "Linear network coding," *IEEE Trans. Inf. Theory*, vol. 49, no. 2, pp. 371–381, Feb. 2003.
[2] Y. Wu, P. A. Chou, and S. Y. Kung, "Information exchange in wireless networks with network coding and physical-layer broadcast," Microsoft Corp., Redmond, WA, USA, Tech. Rep. MSR-TR-2004-78, 2004.
[3] L.-L. Xie, "Network coding and random binning for multi-user channels," in *Proc. 10th Can. Workshop Inf. Theory*, Jun. 2007, pp. 85–88.
[4] W. Chen, Z. Cao, and L. Hanzo, "Maximum Euclidean distance network coded modulation for asymmetric decode-and-forward two-way relaying," *IET Commun.*, vol. 7, no. 10, pp. 988–998, Jul. 2013.

[5] Y. Yang, W. Chen, O. Li, and L. Hanzo, "Variable-rate, variable-power network-coded-QAM/PSK for bi-directional relaying over fading channels," *IEEE Trans. Commun.*, vol. 62, no. 10, pp. 3631–3643, Oct. 2014.
[6] Y. Yang, W. Chen, O. Li, and L. Hanzo, "Joint rate and power adaptation for amplify-and-forward two-way relaying relying on analog network coding," *IEEE Access*, vol. 4, pp. 2465–2478, May 2016.
[7] J. M. Torrance and L. Hanzo, "Optimisation of switching levels for adaptive modulation in slow Rayleigh fading," *Electron. Lett.*, vol. 32, no. 13, pp. 1167–1169, Jun. 1996.
[8] L. Hanzo, S. X. Ng, W. Webb, and T. Keller, *Quadrature Amplitude Modulation: From Basics to Adaptive Trellis-Coded, Turbo-Equalised and Space-Time Coded OFDM, CDMA and MC-CDMA Systems*. Hoboken, NJ, USA: Wiley, 2004.
[9] G. E. Oien, H. Holm, and K. J. Hole, "Impact of channel prediction on adaptive coded modulation performance in Rayleigh fading," *IEEE Trans. Veh. Technol.*, vol. 53, no. 3, pp. 758–769, May 2004.
[10] M.-S. Alouini and A. J. Goldsmith, "Adaptive modulation over Nakagami fading channels," *J. Wireless Commun.*, vol. 13, nos. 1–2, pp. 119–143, May 2000.
[11] A. J. Goldsmith and S.-G. Chua, "Variable-rate variable-power MQAM for fading channels," *IEEE Trans. Commun.*, vol. 45, no. 10, pp. 1218–1230, Oct. 1997.
[12] H. Chen, R. G. Maunder, and L. Hanzo, "Low-complexity multiple-component turbo-decoding-aided hybrid ARQ," *IEEE Trans. Veh. Technol.*, vol. 60, no. 4, pp. 1571–1577, May 2011.
[13] H. A. Ngo, T. D. Nguyen, and L. Hanzo, "Amplify-forward and decode-forward cooperation relying on systematic Luby transform coded hybrid automatic-repeat-request," *IET Commun.*, vol. 5, no. 8, pp. 1096–1106, 2011.
[14] L. Dai and K. B. Letaief, "Throughput maximization of ad-hoc wireless networks using adaptive cooperative diversity and truncated ARQ," *IEEE Trans. Commun.*, vol. 56, no. 11, pp. 1907–1918, Nov. 2008.
[15] J. K. Sundararajan, D. Shah, and M. Médard, "ARQ for network coding," in *Proc. IEEE Int. Symp. Inf. Theory (ISIT)*, Toronto, ON, Canada, Jul. 2008, pp. 1651–1655.
[16] Q. Liu, S. Zhou, and G. B. Giannakis, "Cross-layer combining of adaptive modulation and coding with truncated ARQ over wireless links," *IEEE Trans. Wireless Commun.*, vol. 3, no. 5, pp. 1746–1755, Sep. 2004.
[17] Q. Liu, S. Zhou, and G. B. Giannakis, "Queuing with adaptive modulation and coding over wireless links: Cross-Layer analysis and design," *IEEE Trans. Wireless Commun.*, vol. 4, no. 3, pp. 1142–1153, May 2005.
[18] A. Goldsmith, *Wireless Communications*. New York, NY, USA: Cambridge Univ. Press, 2005.
[19] S. B. Wicker, *Error Control Systems for Digital Communication and Storage*. Englewood Cliffs, NJ, USA: Prentice-Hall, 1995.
[20] K. Cho and D. Yoon, "On the general BER expression of one- and two-dimensional amplitude modulations," *IEEE Trans. Commun.*, vol. 50, no. 7, pp. 1074–1080, Jul. 2002.
[21] A. Doufexi *et al.*, "A comparison of the HIPERLAN/2 and IEEE 802.11a wireless LAN standards," *IEEE Commun. Mag.*, vol. 40, no. 5, pp. 172–180, May 2002.
[22] X. Ge, S. Tu, G. Mao, and C. X. Wang, "5G ultra-dense cellular networks," *IEEE Trans. Wireless Commun.*, vol. 23, no. 1, pp. 72–79, Feb. 2016.
[23] G. L. Stüber, *Principles of Mobile Communication*, 2nd ed. Norwell, MA, USA: Kluwer, 2001.
[24] L. Hanzo, Y. Akhtman, L. Wang, and M. Jiang, *MIMO-OFDM for LTE, WiFi and WiMAX*. Hoboken, NJ, USA: Wiley, 2011.

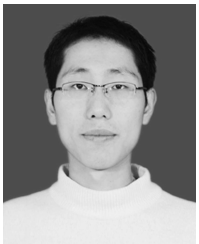

YANPING YANG (S'13) received the B.S. degree in automation and the M.S. degree in electronic engineering from Xidian University, Xi'an, China, in 2008 and 2013, respectively. He is currently pursuing the Ph.D. degree with the National Digital Switching System Engineering and Technological Research and Development Center, Zhengzhou, China, and the Department of Electronic Engineering, Tsinghua University, Beijing, China. His research interests include cognitive radio networks, adaptive modulation & coding and network coding. He is currently a Reviewer of the IEEE JSAC, TVT, CL, and WCL.

WEI CHEN (S'05–M'07–SM'13) received the B.S. degree (Hons.) in operations research and the Ph.D. degree (Hons.) in electronic engineering from Tsinghua University, Beijing, China, in 2002, and 2007, respectively. From 2005 to 2007, he was a Visiting Ph.D. Student with the Hong Kong University of Science and Technology. Since 2007, he has been with the Department of Electronic Engineering, Tsinghua University, where he has been prompted to be Full Professor since 2012, as a special case of early promotion. After the human resource reform with Tsinghua University, he is elected as a Tenured Full Professor of the New Research and Teaching Track in 2015. He also serves as the Deputy Department Head and the University Council Member, and supported by the National 973 Youth Project, the NSFC Excellent Young Investigator Project, the National 10000-Talent Program, the New Century Talent Program of Ministry of Education, and the Beijing Nova Program. He visited the University of Southampton, Telecom ParisTech, and Princeton University in 2010, 2014, and 2016, respectively. He received the thesis awards for B.S. and Ph.D. degrees.

His research interests are in the areas of wireless communications and information theory. He serves as an Editor of the IEEE Transactions on Communications, the IEEE Transactions on Education, the IEEE Wireless Communications Letters, and a Co-Chair of the Communications Theory Symposium in the IEEE Globecom 2017. He served as a Tutorial Co-Chair of the IEEE ICC 2013, a TPC Co-Chair of the IEEE VTC 2011-Spring, and the Symposium Co-Chair of the IEEE ICC, ICCC, CCNC, Chinacom, and WOCC.

Prof. Chen is a recipient of the First Prize of 14th Henry Fok Ying-Tung Young Faculty Award, the Yi-Sheng Mao Beijing Youth Science and Technology Award, the 2010 IEEE Comsoc Asia Pacific Board Best Young Researcher Award, the 2009 IEEE Marconi Prize Paper Award, the 2015 CIE Information Theory New Star Award, the Best Paper Awards at the IEEE ICC 2006, the IEEE IWCLD 2007, and the IEEE SmartGirdComm 2012. He holds the honorary titles of Beijing Outstanding Teacher and the Beijing Outstanding Young Talent. He is the Champion of the First National Young Faculty Teaching Competition, and a winner of National May 1st Medal.

OU LI received the Ph.D. degree from the National Digital Switching System Engineering and Technological Research and Development Center (NDSC), Zhengzhou, China, in 2001. He is currently a Professor with NDSC. His primary research interests include wireless communication technology, wireless sensor network, cognitive radio networks, MIMO, and spectrum sensing.

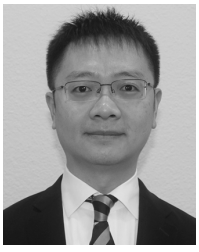

QINGWEN LIU (SM'14) received the B.S. degree in electrical engineering and information science from the University of Science and Technology of China in 2001, the M.S. and Ph.D. degrees with the Department of Electrical and Computer Engineering, University of Minnesota, Minneapolis, in 2003 and 2006, respectively.

He is currently a Professor with the Department of Computer Science and Technology, Tongji University, Shanghai, China. His research interests lie in the areas of communications, signal processing, and networking, with emphasis on cross-layer analysis and design, and quality-of service support for multimedia applications over wired-wireless networks.

LAJOS HANZO (M'91–SM'92–F'04) received the D.Sc. degree in electronics in 1976 and the Ph.D. degree in 1983. In 2009, he was awarded an honorary doctorate by the Technical University of Budapest and the University of Edinburgh in 2015. In 2016, he was admitted to the Hungarian Academy of Science. During his 40-year career in telecommunications he has held various research and academic posts in Hungary, Germany, and the U.K. Since 1986, he has been with the School of Electronics and Computer Science, University of Southampton, U.K., where he holds the Chair in telecommunications. He has successfully supervised 111 Ph.D. students, co-authored 20 John Wiley/IEEE Press books on mobile radio communications totalling in excess of 10,000 pages, and published over 1600 research contributions at the IEEE Xplore, and acted as a TPC and the General Chair of the IEEE conferences, presented keynote lectures, and received a number of distinctions. He is currently directing a 60-strong Academic Research Team, working on a range of research projects in wireless multimedia communications sponsored by industry, the Engineering and Physical Sciences Research Council, U.K., the European Research Council's Advanced Fellow Grant and the Royal Society's Wolfson Research Merit Award. He is also an Enthusiastic Supporter of industrial and an Academic Liaison and he offers a range of industrial courses. He is also a Governor of the IEEE VTS. From 2008 to 2012, he was the Editor-in-Chief of the IEEE Press and a Chaired Professor at Tsinghua University, Beijing. He has over 25,000 citations, and the H-index of 60. He is fellow of FREng, FIEEE, FIET, and EURASIP.

AUTHOR QUERIES

AUTHOR PLEASE ANSWER ALL QUERIES

PLEASE NOTE: We cannot accept new source files as corrections for your paper. If possible, please annotate the PDF proof we have sent you with your corrections and upload it via the Author Gateway. Alternatively, you may send us your corrections in list format. You may also upload revised graphics via the Author Gateway.

AQ:1 = Please confirm the current affiliation of all the authors. Also provide location and postal code for the ''National Digital Switching System Engineering and Technological R&D Center, Tsinghua University, Tongji University, and University of Southampton.''